Oxidation of Metals, Vol. 47, Nos. 3/4, 1997

The Role of Microstructure on Pesting During Oxidation of $MoSi_2$ and $Mo(Si,Al)_2$ at 773 K

Katsuyuki Yanagihara,* Kazimierz Przybylski,† and Toshio Maruyama*

Received April 9, 1996; revised July 31, 1996

The pesting behavior of $MoSi_2$ and $Mo(Si,Al)_2$ has been examined in air at 773 K to clarify the origin and mechanism of pesting phenomena and the effect of aluminum on pesting phenomena. The initial cracks play a much more important role than the grain boundaries and the initial oxide layer in pesting. Mo and Si oxidize to amorphous Mo–Si–O simultaneously with about a 200% volume expansion. Therefore, large stress appears at the cracktips and induce many new cracks. MoO_3 vaporizes from the Mo–Si–O layer on the external surface and crack surfaces causing the oxides in the initial cracks to become porous. Oxygen has a short-circuit path to enter the sample in the cracks. Therefore, the partial pressure of oxygen is sufficiently high to allow oxidation of Mo in the materials. The platelet-like MoO_3 grows on the external surface and also in the cracks. Finally, the sample distintegrates into powder. Pesting of $Mo(Si,Al)_2$ occurs in the same way, however, its rate is much lower than that of $MoSi_2$. The role of Al is to decrease the initial crack density of the samples from the melt. Other effects of Al might be to decrease the oxygen flux toward the oxide-intermetallic interface and to increase the plasticity of the amorphous oxide being formed in the cracks.

KEY WORDS; $MoSi_2$; $Mo(Si,Al)_2$; pesting; disintegration; internal oxidation.

INTRODUCTION

Molybdenum disilicide ($MoSi_2$) is a very promising material because of its high melting point (2303 K), excellent oxidation resistance at temperatures

*Department of Metallurgical Engineering, Faculty of Engineering, Tokyo Institute of Technology, 2-12-1, O-okayama, Meguro-ku, Tokyo 152, Japan.
†Department of Solid State Chemistry, Faculty of Materials Science and Ceramics, University of Mining and Metallurgy, AGH, al.Mickiewicza 30, 30-059 Cracow, Poland.

0030-770X/97/0400-0277$12.50/0

between 1300 K and 2000 K[1–5] and moderate density (6.24 g cm^{-3}). Nevertheless, $MoSi_2$ has several problems to overcome: spalling of the protective SiO_2 scale under thermal cycling and so-called "pesting" in which disintegration occurs during oxidation around 773 K. Grabke and Meier[6] recently reviewed the pesting of several intermetallics including $MoSi_2$. The present authors[7–9] have reported the results of high-temperature oxidation of Mo-Si-X (X = Al, Ta, Ti, Zr, and Y) intermetallics, and evaluated the effect of the third element X on the oxidation rate and on the suppression of crystallization of amorphous silica scale which induces scale spalling.

The present paper deals with pesting. Fitzer[10] first described the phenomenon of $MoSi_2$ disintegration into powder and named it "pest" in 1955. Many researchers have studied this phenomenon,[6,11–21] but the origin and the mechanism of pesting are still open to discussion. The salient points are enumerated in the following.

1. The role of grain boundaries and initial microcracks and pores in the pesting behavior.
2. The temperature dependence of pesting rate.
3. The mechanism of distintegration into powder.
4. The effect of third elements on pesting.

Fitzer,[10] Meschter[5] and other workers[11,12,18,19] concluded that the pesting phenomenon was not an intrinsic property of $MoSi_2$ and that it required the presence of initial microcracks and pores in the material. McKamey *et al.*[11] and Berztiss *et al.*[12] demonstrated that simultaneous oxidation of Mo and Si at the initial cracks with a large volume expansion induced the pesting phenomenon of $MoSi_2$. Berztiss *et al.*[12] reported that cast $MoSi_2$ disintegrated into powder, but single-crystal and crack-free polycrystal $MoSi_2$ prepared by hot isostatic pressing (HIP) did not disintegrate. However, Chou and Nieh[13–17] showed that $MoSi_2$ prepared by hot pressing underwent severe pesting at 773 K and single crystals of $MoSi_2$ also disintegrated into small $MoSi_2$ crystals, powdery MoO_3 whiskers and SiO_2 clusters. They concluded that simultaneous oxidation of Mo and Si with a large volume expansion at grain boundaries was the main cause of pesting. McKamey *et al.*[11] reported that polycrystalline $MoSi_2$ with excess Si was able to form a protective SiO_2 scale and showed no indication of pesting, even at sample densities as low as 60% theoretical density. Berkowitz-Mattuck *et al.*[18,19] suggested that stress-enhanced oxidation at the tips of Griffith flaws occurred, the stresses being introduced by cooling from the melt. According to these authors,[19] the absence of pesting phenomenon above 873 K was due to plastic deformation of the $MoSi_2$ matrix that tended to reduce the stress concentration.

Cook *et al.*[2] found that a $MoSi_2$-30 vol.% SiC composite did not disintegrate after thermal cycling between 1773 K and room temperature

to introduce cracks, but the composite distintegrated severely during oxidation at 773 K. Their result indicated that single-crystal and crack-free polycrystalline $MoSi_2$ should undergo pesting after thermal cycling, because of crack formation due to the thermal stress and the difference of thermal expansion coefficients of matrix and scale or matrix and reinforcements. Considering the commercial use of $MoSi_2$ composites, the absence of cracks in the initial material does not guarantee its resistance to pesting.

Mueller *et al.*[20] demonstrated that small additions of Ge prevented pesting of $MoSi_2$ by stabilizing the protective SiO_2 layer. Cook *et al.*[2] noted that $MoSi_2 + MB_2$ (M = Ti, Zr and Hf) composite did not disintegrate during oxidation at 773 K, even after thermal cycling between 1773 K and room temperature. The present authors[21] have studied the pesting kinetics of Mo–Si–X (X = Al, Ta, Ti, Zr, and Y) intemetallics to evaluate the third-element effect. The third elements whose affinity for oxygen are less than that of Si (i.e., Ta) had no effect on the suppression of pesting. However, the third elements whose affinites for oxygen are stronger than that of Si (i.e., Al, Ti, Zr, and Y) prevented pesting. These results indicate that third elements may have a great effect on the pesting rate. From thermodynamic considerations, selective oxidation should occur at the grain boundaries. The present authors have concluded[21] that the main cause of pesting was the internal stress caused by volume expansion accompanying selective oxidation at the grain boundaries. To prove this conclusion, it is necessary to identify the oxide which forms at grain boundaries during oxidation.

In the present study, the pesting behavior of $MoSi_2$ and $Mo(Si,Al)_2$ has been examined in air at 773 K to clarify the origin and mechanism of pesting phenomenon and the effect of aluminum on it.

EXPERIMENTAL PROCEDURES

The $MoSi_2$ and $Mo(Si,Al)_2$ intermetallics were prepared by arc-melting of plates of constituent elements Mo, Si, and Al (99.9 mass %) in an argon atmosphere. Figure 1 shows a tentative phase diagram of the Mo–Si–Al system at 773 K. The points of Y and Z in Fig. 1 represent the compositions of $MoSi_2$ (Mo = 33.3 mol.% and Si = 66.7 mol.%) and $Mo(Si,Al)_2$ (Mo = 33.3 mol.%, Si = 56.7 mol.% and Al = 10 mol.%), respectively. The resulting buttons were cut into pieces ($10 \times 7 \times 1$ mm). The surfaces of the samples were polished using 800-grit SiC paper, followed by ultrasonic cleaning in acetone.

Oxidation was conducted at 773 K in air. The samples were placed in an Al_2O_3 crucible and heated by an electrical-resistance furnace. The surfaces

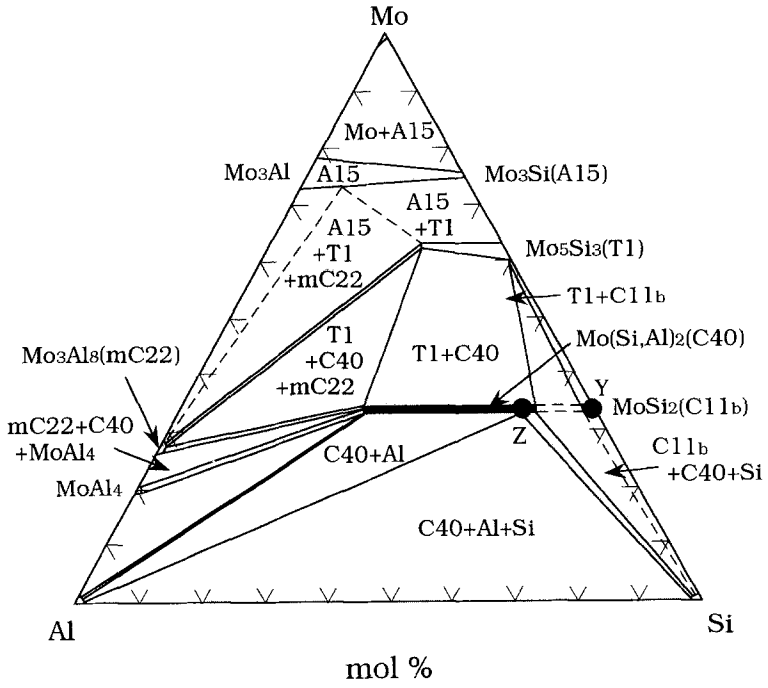

Fig. 1. Tentative phase diagram of the Mo–Si–Al system at 773 K.

of oxidized samples were examined by X-ray diffraction (XRD: SEIFERT-FPM XRD7) with 2 deg incidence and scanning electron microscopy (SEM: JOEL-JSM5400) with energy dispersive spectroscopy (EDS) analysis. All samples were fractured after quenching in liquid nitrogen and the cross sections were examined by SEM with EDS analysis. As arc-melted and oxidized $Mo(Si,Al)_2$ were studied by conventional transmission electron microscopy (TEM), EDS and selected area diffraction (SAD) using a Philips CM 20 equipped with a Link eXL EDS system. The samples, which were all oriented parallel to the scale-intermetallic interface, were prepared by first thinning the arc-melted and oxidized samples from one side by grinding to a thickness of 0.3 mm. An ultrasonic drill was employed to cut out 3 mm diam disks of the oxide-intermetallic layered composite. The 3-mm disks were thinned by dimpling on a Gatan Dimpler and ion-milled on a Gatan DuoMill 600 with 5 kV argon ions at an incidence angle of 15 deg. This technique produces, ideally, an electron-transparent section of the samples. Oxides on $MoSi_2$ and $Mo(Si,Al)_2$ oxidized for 36 ks were stripped from the external surfaces, using an extraction replica method. The thickness of most oxides was sufficient for direct TEM-SAD observation.

RESULTS

Figure 2 shows the external surfaces of $MoSi_2$ and $Mo(Si,Al)_2$ oxidized at 773 K for 36 ks. Both samples have preserved the initial shape without disintegration. Platelet-like oxides formed on the external surface, especially along the initial cracks, pores and polishing scratches (A). Cluster-like oxide also exists in the cracks of $MoSi_2$ (B). EDS analysis shows that the platelet-like oxides and the cluster-like oxide are composed mainly of Mo-oxide and Si-oxide, respectively. The cluster-like oxide was not detected on $Mo(Si,Al)_2$. More and larger platelet-like oxide exists on $MoSi_2$ in comparison with $Mo(Si,Al)_2$. The XRD analysis from external surfaces of both samples exhibited sharp diffraction peaks from the matrix and weak peaks of MoO_3. The EDS analysis of the scales on $MoSi_2$ indicated the formation of Mo–Si–O oxide and on $Mo(Si,Al)_2$ indicated the formation of Mo–Si–Al–O whose XRD peaks were not detected. Therefore, the Mo–Si–O layer on $MoSi_2$ and the Mo–Si–Al–O layer on $Mo(Si,Al)_2$ were in an amorphous state.

The oxides on external surfaces of $MoSi_2$ and $Mo(Si,Al)_2$ oxidized for 36 ks were stripped by an extraction-replica method. Figure 3 exhibits TEM bright-field images and electron diffraction patterns of the platelet-like oxide on both samples. The platelet-like oxide is thin enough to be electron transparent. The EDS analysis shows that the platelet-like oxide was composed of Mo-oxide without Si or Al. The platelet-like oxides on $MoSi_2$ and $Mo(Si,Al)_2$ were identified by electron diffraction as single crystals of MoO_3 with an orthorhombic structure.

Figure 4 displays cross sections of $MoSi_2$ oxidized at 773 K for 36 ks. The platelet-like MoO_3 was observed in $MoSi_2$ (B) and the oxide grows with increasing oxidation time. The initial pores were heavily oxidized. Another type of porous oxide is found in the initial cracks (C). The EDS analysis shows the ratio of Mo–Si of the porous oxide is close to that of $MoSi_2$ with slightly smaller Mo content. It might be reasonably assumed that this oxide formed during the simultaneous oxidation of Mo and Si, and MoO_3 vaporized in the subsequent oxidation period. Therefore, this oxide is porous. The cluster-like oxide in Fig. 2 is the same one as the porous oxide (C) in Fig. 4. One grain has much oxide but the neighboring one has no oxide at all (A) even after oxidation for 36 ks. No Mo-rich phase, for example Mo_5Si_3, was found around the oxide. Mo oxidized simultaneously with Si in the samples. Cross sections of $Mo(Si,Al)_2$ oxidized for 36 ks are presented in Fig. 5. The platelet-like MoO_3 (A) and another type of porous oxide (B) exist as in the case of $MoSi_2$. However, the amount of oxide in $Mo(Si,Al)_2$ is much less in comparison with that in $MoSi_2$. Figure 5 shows clearly that the platelet-like MoO_3 starts to grow from the porous oxide in the initial

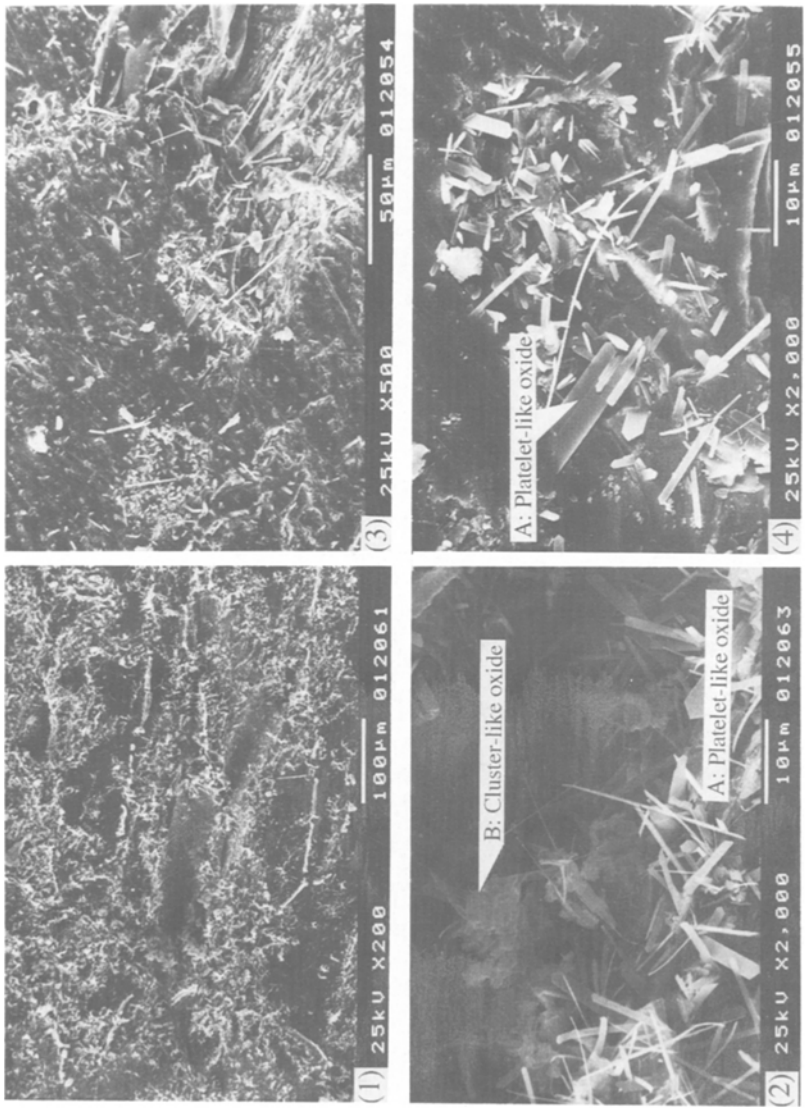

Fig. 2. Surface appearance of $MoSi_2$ (1), (2) and $Mo(Si,Al)_2$ (3), (4) oxidized at 773 K for 36 ks.

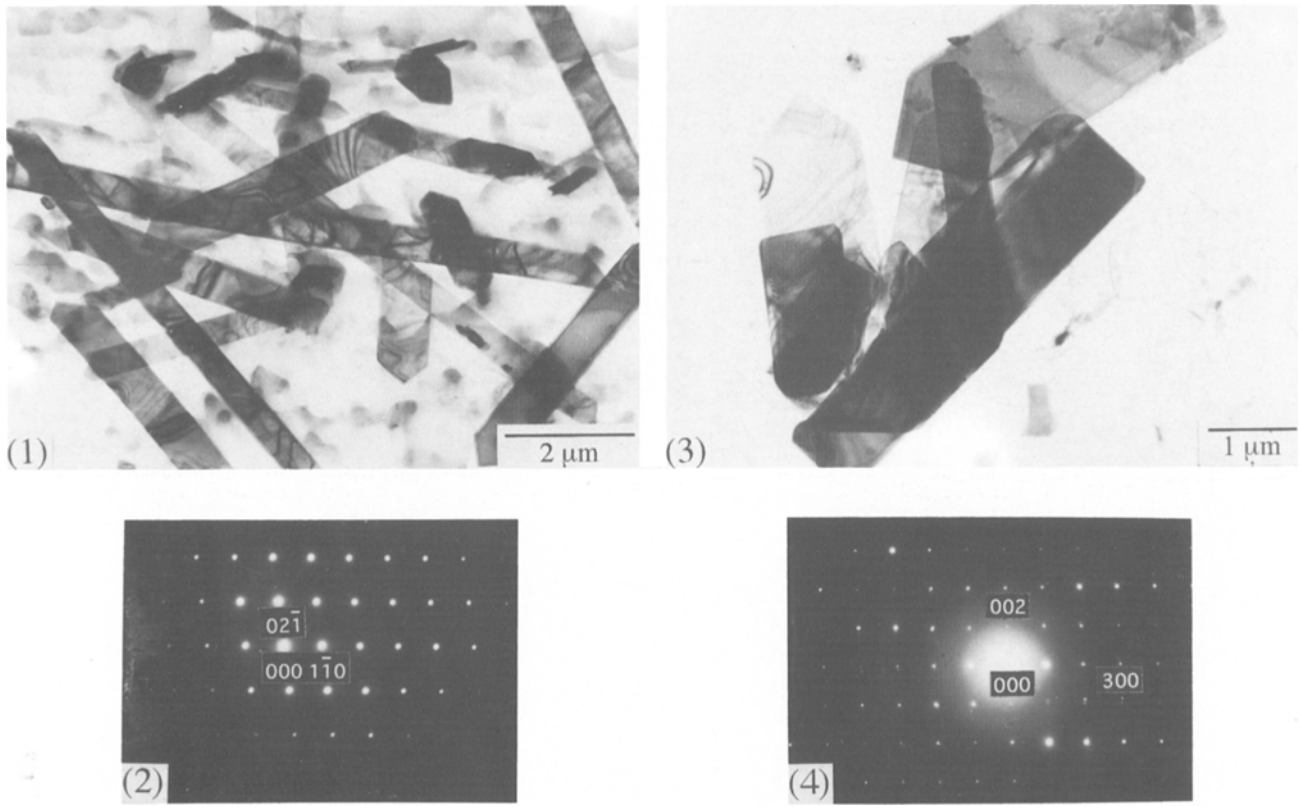

Fig. 3. TEM bright-field images and electron-diffraction patterns of platelet-like MoO_3 formed on $MoSi_2$ (1), (2) and $Mo(Si,Al)_2$ (3), (4) oxidized at 773 K for 36 ks.

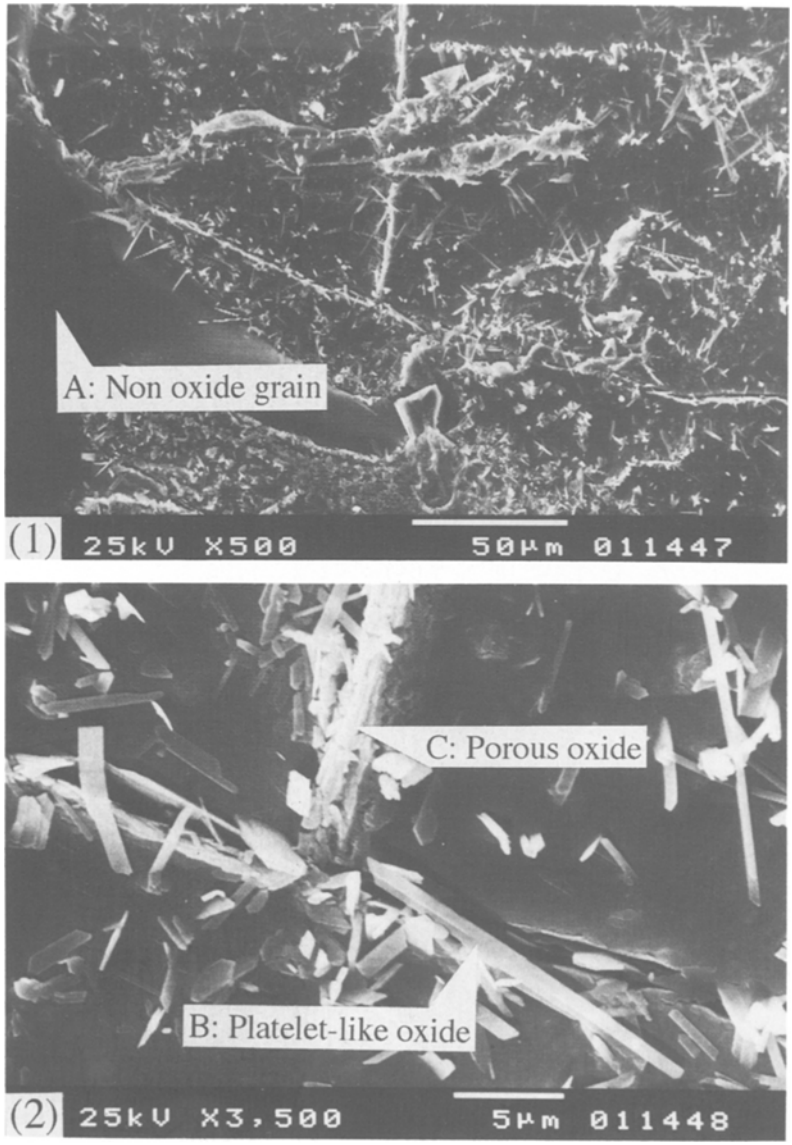

Fig. 4. Cross sections of $MoSi_2$ oxidized at 773 K for 36 ks.

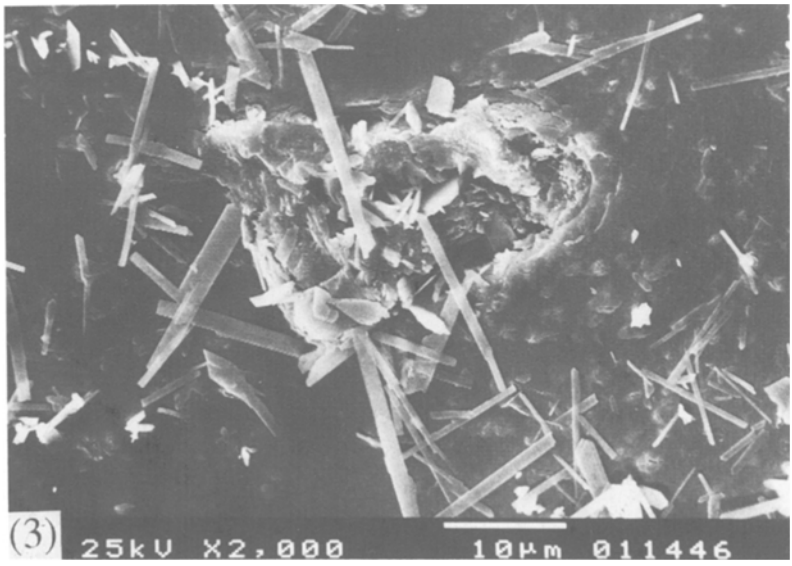

Fig. 4. Continued.

crack and the Mo–Si–Al–O oxide. Figures 5 also indicates that this area has already split into two crack surfaces by pesting. The platelet-like MoO_3 grows vertically about 5 μm of length in $Mo(Si,Al)_2$. The length of the platelet-like MoO_3 suggests that the width of the crack is more than 5 μm.

Figure 6 shows bright-field images of $Mo(Si,Al)_2$ and electron-diffraction patterns of the particle in the oxide layer. The layer whose width is about 0.3 μm exists within the matrix in the arc-melted $Mo(Si,Al)_2$ (B). Many small particles are observed in the layer. Judging from the overlapping of oxide layer and matrix, the adherence of the oxide layer to the matrix is excellent. The EDS analysis indicated that the black particles (C) and bright part (D) are Al_2O_3 or a mixture of Al_2O_3 and mullite, respectively. Electron diffraction identified that C is a single crystal of α-Al_2O_3. After 288 ks oxidation, there is no sign of pesting at this layer, and the adherence of the layer to the matrix is excellent. This result indicates that the initial oxide layer is not the site of pesting.

4 DISCUSSION

The Site of Internal Oxidation

The average grain size of cast samples is over 400 μm, whereas that of the samples which are prepared by HIP or hot pressing is about 20 μm.[11,12]

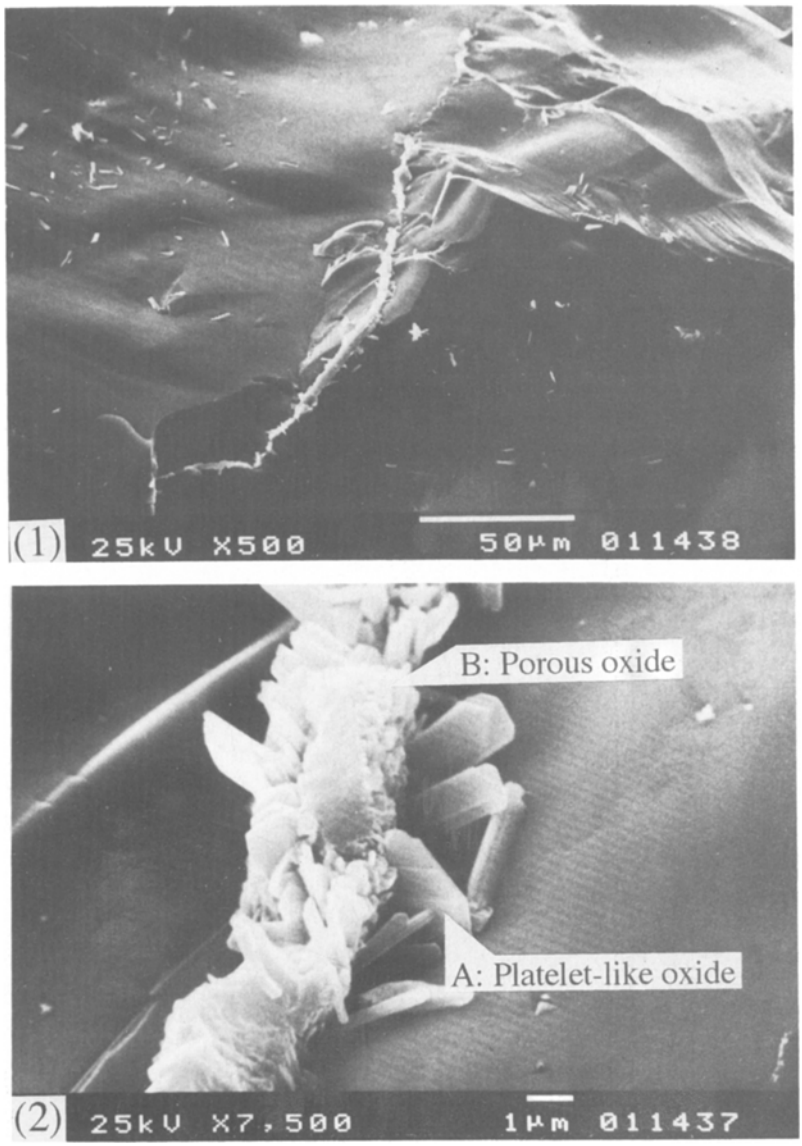

Fig. 5. Cross sections of $Mo(Si,Al)_2$ oxidized at 773 K for 36 ks.

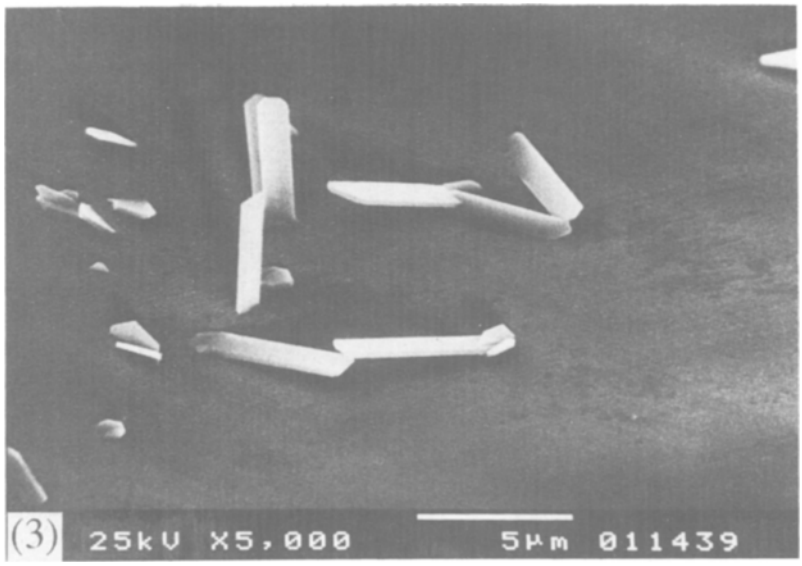

Fig. 5. Continued.

Therefore, the area of grain boundaries per unit volume in arc-melted samples is much smaller than that of the samples prepared by HIP or hot pressing. If internal oxidation at grain boundaries were the main reason of pesting, the pesting rates should increase with decreasing grain size. However, Berztiss *et al.*[12] reported that crack-free polycrystalline $MoSi_2$ prepared by HIP did not disintegrate and that initial cracks and pores were the site of internal oxidation which induced disintegration. McKamey *et al.*[11] concluded that grain boundaries were not the main site of pesting because many cracks occurred in the grains. On the other hand, Chou and Nieh[13–17] described that simultaneous oxidation of Mo and Si at grain boundaries was the main reason of pesting. In this study, the cross section showed that one grain may have much oxide and the neighboring one may have no oxide at all (Fig. 4). This clearly indicates that grain boundary is not the site of internal oxidation which induces distintegration. As shown in Fig. 6, the arc-melted samples have an initial oxide layer inside. It can be reasonably assumed that the oxide layer formed on the external surface during arc-melting process and it was subsequently swallowed up during remelting. This initial oxide layer is a peculiar feature of the arc-melted samples. After 288 ks oxidation, there is no sign of pesting in the vicinity of the oxide layer. Neither is the initial oxide layer the site of internal oxidation which causes sample disintegration. These results indicate that the initial cracks play a

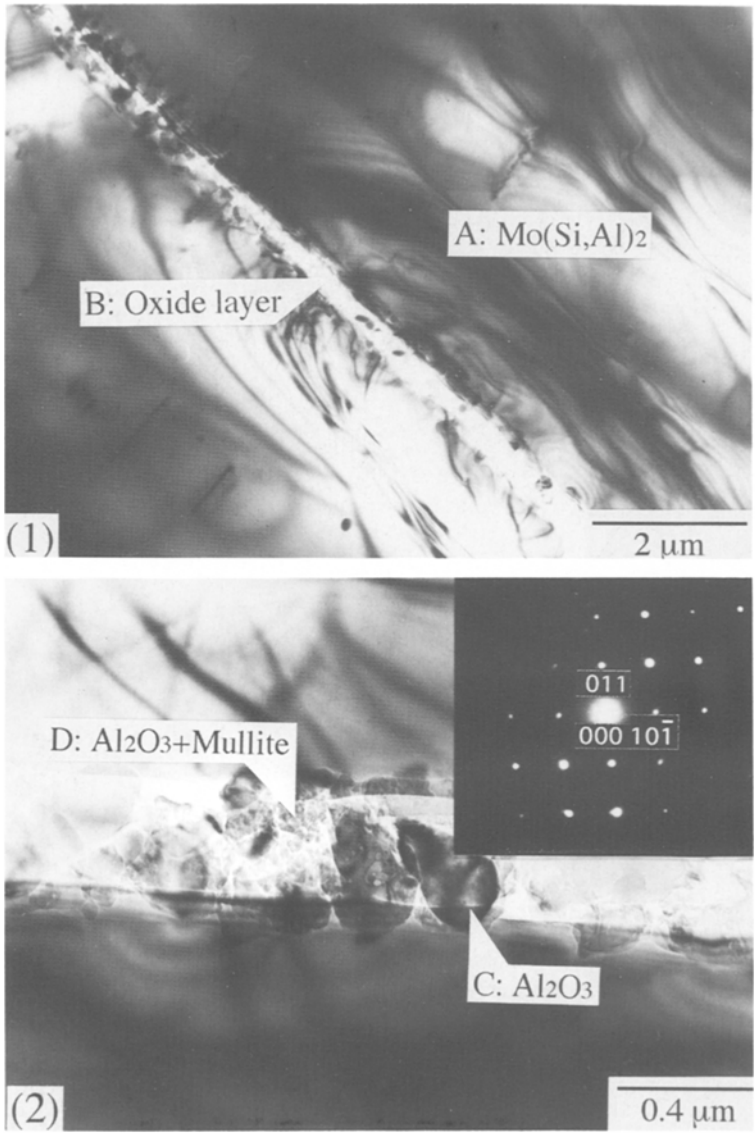

Fig. 6. TEM bright-field images and electron-diffraction patterns of the particle in the layer of $Mo(Si,Al)_2$: as arc-melted (1), (2) and oxidized at 773 K for 288 ks (3).

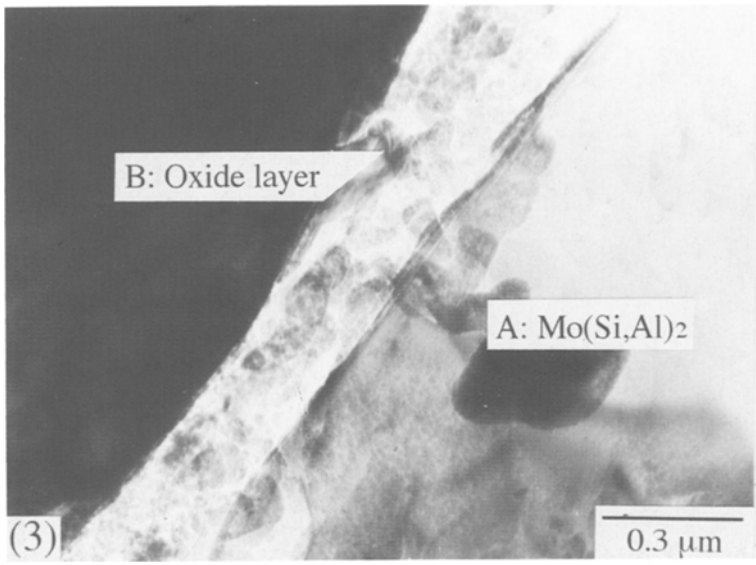

Fig. 6. Continued.

much more important role in pesting phenomenon than grain boundaries and the initial oxide layer.

Mechanism of Pesting Phenomenon

From thermodynamic considerations,[21] it follows that Si in $MoSi_2$ should be selectively oxidized to SiO_2 because its affinity for oxygen is much greater than that of Mo. Similarly, Al should oxidize selectively in $Mo(Si,Al)_2$.[21] However, no Mo-rich phase was found around the internal oxide. This result indicates that oxidation of Mo and Si or Mo, Si and Al in the intermetallics occurred simultaneously. Berztiss *et al.*[12] reported that Mo and Si oxidized simultaneouly during oxidation at 733 K because the ratio of Mo and Si in the scale is close to that of matrix, which is in agreement with the present results. One possible explanation is that the diffusivity of elements in $MoSi_2$ and $Mo(Si,Al)_2$ is too low around 733 K to obey the thermodynamics. Consequently, the oxidation kinetics controls the pesting phenomenon.

Berztiss *et al.*[12] suggested that platelet-like MoO_3 grows by vapor-deposition. According to their suggestion, the growth of platelet-like MoO_3 does not generate any stress to disintegrate the sample. The amorphous Mo–Si–O and Mo–Si–Al–O oxides which were formed in this study have the

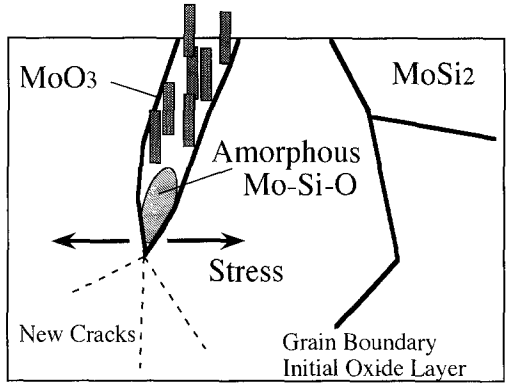

Fig. 7. Pesting model of $MoSi_2$.

composition of metal elements close to that in the initial intermetallics. It means that the vaporization of MoO_3 does not play a singificant role. Simultaneous oxidation of Mo and Si or Mo, Si and Al are described as follows:

$$2MoSi_2 + 7O_2 \rightarrow 2MoO_3 + 4SiO_2 \quad (1)$$

$$40Mo(Si_{0.85}, Al_{0.15})_2 + 137O_2 \rightarrow 40MoO_3 + 68SiO_2 + 6Al_2O_3 \quad (2)$$

The calculated volume change involved in reaction (1) is about 212 vol.%, and that in reaction (2) is 190 vol.%. In the real oxidation process, the reaction products are amorphous Mo–Si–O and Mo–Si–Al–O, respectively. It can be reasonably assumed that the volume expansion during the simultaneous oxidation of both samples is about 200 vol.%. The simultaneous oxidation generates the internal stress that leads to distintegration.

Figure 7 shows the model for pesting of $MoSi_2$. $MoSi_2$ oxidizes on the external surface and also in the cracks. However, grain boundaries and the initial oxide layer are not the site of internal oxidation. Simultaneous oxidation of Mo and Si is accompanied by about a 200% volume increase. Therefore, large stress appears at the cracktips and induces many new cracks. MoO_3 vaporizes from the Mo–Si–O layer formed on the external surface or crack surfaces making the oxide in the initial cracks porous as shown in Figs. 4 and 5. As a consequence, oxygen has a short-circuit path to enter the sample in the cracks. Therefore, the partial pressure of oxygen remains high enough to allow oxidation of Mo in the materials. The platelet-like MoO_3 grows on the external surface and also in the cracks as shown in Figs. 2–5. Finally, the sample disintegrates into powder. Pesting of $Mo(Si,Al)_2$ occurs in the same way.

Effect of the Third Element

The pesting rate of $Mo(Si,Al)_2$ is much lower than that of $MoSi_2$. The present authors proposed[21] that the pesting rates depended on the volume-expansion ratio during selective oxidation of Si to SiO_2 in $MoSi_2$ and Al to Al_2O_3 in $Mo(Si,Al)_2$. However, the present results show the occurrence of simultaneous oxidation. The main differences of $MoSi_2$ and $Mo(Si,Al)_2$ are initial crack density of the samples and content of Al. The $MoSi_2$ sample contains many cracks, whereas the $Mo(Si,Al)_2$ sample contains only a few cracks after arc-melting under the same conditions. As discussed, the cracks are the sites of internal oxidation inducing distintegration. Therefore, the initial crack density should have a great effect on the pesting rate. Nevertheless, the pesting of $Mo(Si,Al)_2$ is not severe even around the initial cracks. In our previous works,[21] $(Mo,Ta)Si_2$ with a few cracks disintegrated into powder as severely as $MoSi_2$. McKamey *et al.*[11] reported that polycrystalline $MoSi_2$ with excess Si was able to form a protective SiO_2 scale and showed no indication of pesting, even at sample densities as low as 60% theoretical density. Their samples should have many open pores which play the same role as initial microcracks. Thus the initial crack density is one parameter affecting the pesting rate, but not the dominant one.

Berkowitz-Mattuc *et al.*[18] reported that the pesting rate is extremely sensitive to oxygen pressure. They suggested that the oxygen flux through the oxide which formed in the cracks controlled the pesting rate. Considering the effects of small addition of Ge[20] and excess Si[11] in $MoSi_2$, pesting of $MoSi_2$ exists on the delicate balance between the oxygen flux and silicon flux toward the oxide-intermetallics interface. It is possible to consider that the effect of Al on pesting is to decrease the oxygen flux in the Mo–Si–Al–O layer in comparison with that in the Mo–Si–O layer. As a result, pesting is suppressed.

Another reason might be the plasticity of the oxide which formed by simultaneous oxidation. The melting point of MoO_3 is 1068 K. The softening temperature of amorphous Mo–Si–O should be lower. Addition of the third-element oxide, for example B_2O_3 or Al_2O_3, in amorphous Mo–Si–O, brings about a decrease of the softening temperature due to which the amorphous Mo–Si–X–O might be sufficiently plastic at 773 K. Thus the stress which appears at the cracktips decreases and the pesting phenomenon is suppressed.

The Temperature Dependence of the Pesting Phenomenon

Pesting is not observed at 873 K.[12,17,21] Above 1273 K, MoO_3 vaporizes, and diffusion of Si is rapid enough to form a continuous protective oxide scale.[12] Berztiss *et al.*[12] reported that internal oxidation of Si occurred above

873 K and that MoO_3 was retained on $MoSi_2$ surfaces up to 1073 K. This means the volatility of MoO_3 is not severe even at 1073 K. In the case of the selective oxidation of Si, the volume expansion is calculated to be +85.6%.[21] The volume expansion is probably significant and generates a large internal stress resulting in disintegration of $MoSi_2$. Berkowitz-Mattuck *et al.*[19] described that the absence of pesting above 873 K by plastic deformation of the matrix, which reduced stress concentration. However, the ductile-brittle transformation temperature (DBTT) of $MoSi_2$ has been reported as about 1300 K.[22] In a recent study, Aikin[23] concluded the DBTT of $MoSi_2$ was about 1600 K. The large stress which generates disintegration cannot be reduced at temperatures as low as 773 K. The plasticity of the oxide plays an important role in the temperature dependence of pesting phenomenon. The viscosity of the Mo–Si–O decreases with increasing temperature, and the amorphous Mo–Si–O is probably plastic above 873 K. Thus the stress which appears at the cracktips decreases and the pesting phenomenon is suppressed.

CONCLUSIONS

The pesting behavior of $MoSi_2$ and $Mo(Si,Al)_2$ has been examined in air at 773 K. The initial cracks play a much more important role in pesting phenomenon that grain boundaries and the initial oxide layer. Simultaneous oxidation of Mo and Si generates large stress at the cracktips and induces many new cracks. The platelet-like MoO_3 grows on the external surface and also in the cracks. Oxygen has a short-circuit path to enter the sample in the cracks. Therefore, the partial pressure of oxygen is sufficiently high to allow oxidation of Mo. The pesting rate of $Mo(Si,Al)_2$ is much lower than that of $MoSi_2$. The effect of Al on preventing the pesting phenomenon is to decrease the initial crack density of the samples from the melt. Other possible effects of Al are to decrease the oxygen flux toward the oxide-intermetallics interface and to increase the plasticity of the amorphous oxide formed in the cracks.

ACKNOWLEDGMENTS

One of the authors (K.Y.) expresses his appreciation for the opportunity of a five month study period at the University of Mining and Metallurgy, AGH in Cracow as a Research Fellow of the Japan Society for Promotion of Science. The authors gratefully acknowledge financial support for this researches from the Faculty of Materials Science and Ceramics, University of Mining and Metallurgy, AGH.

REFERENCES

1. E. W. Lee, J. Cook, A. Khan, R. Mahapatra and J. Waldman, *J. Met.* **43**, 54 (1991).
2. J. Cook, A. Khan, E. Lee and R. Mahapatra, *Materials Science and Engineering* **A155**, 183 (1992).
3. J. Schlichting, *High Temperatures–High Pressures*, **14**, 717 (1982).
4. A. K. Vasudevan and J. J. Petrovic, *Materials Science and Engineering* **A155**, 1 (1992).
5. P. J. Meschter, *Metall. Trans.* **23A**, 1763 (1992).
6. H. J. Grabke and G. H. Meier, *Oxidation of Metals* **44**, 147 (1995).
7. T. Maruyama, K. Yanagihara and K. Nagata, *Corrosion Science* **35**, 939 (1993).
8. K. Yanagihara, T. Maruyama and K. Nagata, *Materials Transactions, JIM* **34**, 1200 (1993).
9. K. Yanagihara, T. Maruyama and K. Nagata, *Intermetallics* **3**, 243 (1995).
10. E. Fitzer, *Proc. 2nd Plansee Semin.* 56 (1955).
11. C. G. McKamey, P. F. Tortorelli, J. H. DeVan, and C. A. Carmichael, *L. Mate. Res.* **7**, 2747 (1992).
12. D. A. Berztiss, R. A. Cerchiara, E. A. Gulbransen, F. S. Pettit, and G. H. Meier, *Materials Science and Engineering*, **A155**, 165 (1992).
13. T. C. Chou and T. G. Nieh, *JOM* 15 December (1993).
14. T. C. Chou and T. G. Nieh, *Mat. Res. Symp. Proc.* **288**, (1993).
15. T. C. Chou and T. G. Nieh, *Scripta Metallurgicaet Materialia*, **27**, 1637 (1992).
16. T. C. Chou and T. G. Nieh, *Scripta Metallurgicaet Materialia* **26**, 19 (1992).
17. T. C. Chou and T. G. Nieh, *J. Mater. Res.* **8**, 214 (1993).
18. J. B. Berkowitz-Mattuck, P. E. Blackurn, and E. J. Felten, *Trans. Met. Soc. AIME* **233**, 1093 (1965).
19. J. B. Berkowitz-Mattuck, M. Rossetti, and D. W. Lee, *Metall. Trans.* **1**, 479 (1970).
20. A. Mueller, G. Wang, R. A. Rapp, and E. L. Courtright, *J. Electrochem. Soc.* **139**, 1266 (1992).
21. K. Yanagihara, T. Maruyama, and K. Nagata, *Intermetallics*, **4**, 5133 (1996).
22. Y. Umakoshi, T. Sakagami, T. Hirano, and Y. Yamane, *Acta Metall.* **38**, 909 (1990).
23. R. M. Aikin Jr., *Scripta Metall.* **26**, 1025 (1992).